

Water Vapor and Cloud Detection Validation for Aqua Using Raman Lidars and AERI and the AWEX-G Validation Experiment

Annual Report April 2004

David Whiteman, Belay Demoz, Frank Schmidlin, NASA/GSFC,
Greenbelt, MD, 20771

Zhien Wang, Igor Veselovskii, Wallace McMillan, Ray Hoff, Felicita
Russo, Scott Hannon, University of Maryland, Baltimore County,
Baltimore, MD

Larry Miloshevich, National Center for Atmospheric Research,
Boulder, CO

Barry Lesht, DOE/Argonne National Laboratory, Chicago, IL
Holger Vömel, University of Colorado, Boulder, CO

Gary Jedlovec, NASA/Marshall Space Flight Center, Huntsville, AL

Dan DeSlover, University of Wisconsin, Madison WI

Martin Cadirola, Ecotronics Ventures, LLC, Germantown, MD

Contact: David Whiteman, NASA/GSFC, Code 912, Greenbelt, MD
20771, 301 614-6703, david.n.whiteman@nasa.gov

Abstract

The early work in this investigation focused on the use of Raman lidar, radiosonde and AERI measurements for AIRS validation measurements as was reported in last year's annual report. That report revealed at times large unexplained differences in various validation datasets being used for AIRS validation. Because of this, the AIRS Water Vapor Experiment-Ground (AWEX-G) was proposed, funded and executed. We review some early validation measurements that helped to motivate AWEX-G and then provide preliminary results from that field campaign that occurred October 27 - November 19, 2003 at the Southern Great Plains site of the Department of Energy's Atmospheric Radiation Measurements program.

1 Introduction and Background

The early work in this investigation involved the use of Raman lidar, AERI, and radiosonde measurements of water vapor, temperature, pressure and clouds to study and validate Aqua retrievals of water vapor and to develop cloud particle size retrieval techniques. According to the needs of the Aqua activity, the first 18 months of this activity were focused on combined ground-based measurements during nighttime overpasses of the Aqua satellite in order to validate Aqua water vapor and temperature profiles. Two measurement campaigns were completed. The first of these occurred at NASA/GSFC in Greenbelt, Maryland and spanned September 5 – November 3, 2002 with 26 nighttime overpasses of the Aqua satellite being covered. The second of these campaigns occurred at the University of Maryland Baltimore County and spanned January 8 – January 27, 2003. In addition to the previously mentioned instrumentation, the ground-based BBAERI (Baltimore Bomem AERI), the Atmospheric Lidar Experiment (ALEX) Raman Lidar and the Elastic Lidar Facility (ELF) backscatter lidar made measurements during this second campaign. The preliminary SRL water vapor measurements from this second campaign are being compared with ALEX Raman Lidar measurements for calibration of that system.

Results from early Aqua validation activities such as these demonstrated that a large uncertainty in UTH measurements existed among the measurement technologies in use. The magnitude of the uncertainties in many of the validation datasets complicated the AIRS spectroscopy validation effort and helped to motivate the AIRS Water Vapor Experiment-Ground (AWEX-G) that occupied the bulk of this past year's activity. Some examples of the early comparisons of AIRS observations and validation measurements will now be presented.

2 Review of selected AIRS validation measurements

Figure 1 presents an early comparison of the brightness temperature differences between AIRS measurements and the output of the version of the AIRS fast radiative transfer model, SARTA, that was in use in early 2003. These comparisons will be referred to as Obs-Calc to signify the difference between AIRS observations and calculations of SARTA. The water vapor inputs to the model were provided by the NASA/GSFC Scanning Raman Lidar (SRL) and Vaisala RS-90 radiosondes. The SRL measurements were acquired at GSFC in the fall of 2002 and did not account for the temperature dependence of the Raman spectrum of water vapor nor for the lidar overlap function. Those corrections are now being made in the SRL analysis and resolve much of the dis-

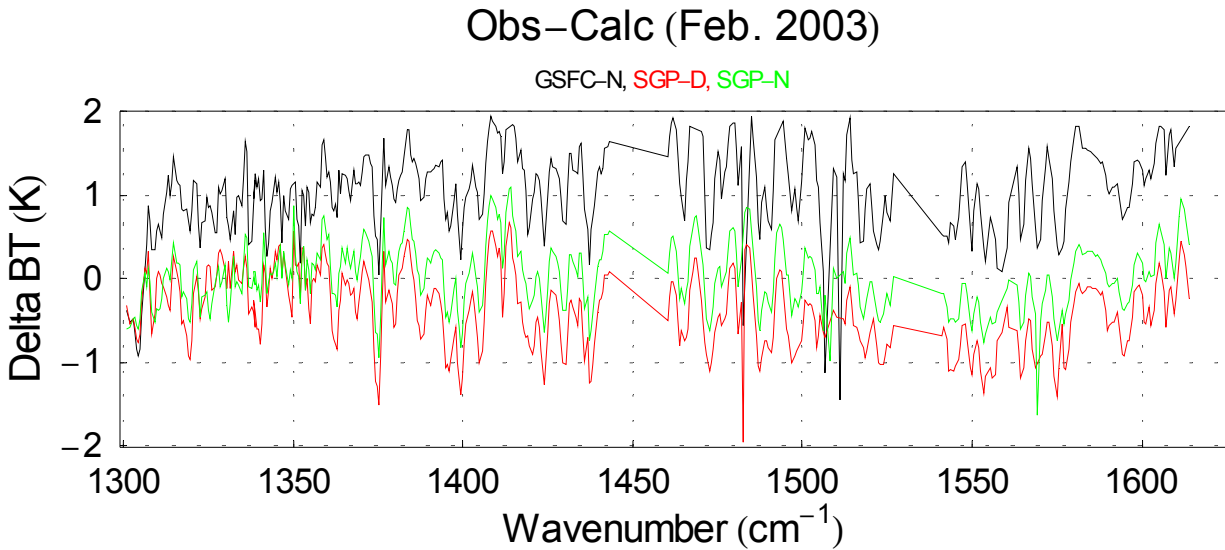


Figure 1: An example of AIRS Obs-Calc analysis using SRL and RS-90 data from early 2003. This is presented to give an idea of some of the uncertainties that existed in the validation activity at that time. Both the AIRS fast model and the analysis of the SRL data have been updated since this comparison was first performed.

agreement shown in the figure. Those corrections will be described later in this document. Also presented in the figure is a comparison with RS-90 measurements acquired in the fall of 2002 from the Department of Energy’s (DOE) Southern Great Plains (SGP) site in northern Oklahoma. These sonde comparisons have been separated into day and night launches to study any diurnal effects that might be present.

Several points can be made from figure 1. The first is that a 25% range in water vapor calibration is implied by the ~2K uncertainty observed through most of the water band [5], which covers approximately 1300 - 1600 cm^{-1} . It should be mentioned here that Obs-Calc comparisons based on other validation datasets (not shown), some acquired using Vaisala RS-90s as well, implied even larger uncertainties in water vapor calibration. The correlation of the high frequency structure in all the measurements seen in figure 1 implied, considering that the radiosonde and lidar measurements were acquired from different locations and at different times, that there likely were errors in the water vapor spectroscopy being used in the forward model. Thus it seemed likely that errors existed in the AIRS fast model but there were many questions about what should be used as validation data to help resolve these differences. The questions of what to use for AIRS validation seemed largest in the upper troposphere where cold temperatures make reliable radiosonde measurements of water vapor more difficult and since the disagreement of the measurements shown in figure 1 was largest in the higher wavenumber portion of the water band. However, there was a history within the DOE Atmospheric Radiations Measurement (ARM) program of achieving good agreement among various upper tropospheric water vapor sensors. This agreement was achieved in the AFWEX (ARM FIRE [First International Satellite Cloud Climatology Project Regional Experiment Water

Vapor Experiment] field campaign [2] held at the SGP site in November-December, 2000 was called AFWEX and will be described next.

3 AFWEX - ARM FIRE Water Vapor Experiment

The Department of Energy's Atmospheric Radiation Measurements program is designed to reduce the uncertainty in measuring and modeling atmospheric radiative fluxes. The dominant role that water vapor plays in atmospheric radiation calculations requires careful research into water vapor measurement accuracies. These requirements have translated into a series of ARM Water Vapor IOPs [4] which focussed on lower level water vapor measurements and AFWEX, which focused on the upper tropospheric water vapor measurement capabilities of various remote and in-situ sensors. AFWEX was staged at the ARM Southern Great Plains (SGP) Cloud and Radiation Testbed (CART) site in northern Oklahoma during November-December, 2000. The instrumentation deployed for AFWEX included ground-based lidars: NASA/GSFC Scanning Raman Lidar and the DOE Raman Lidar, various radiosondes: Vaisala RS-80H, SnowWhite chilled mirror hygrometer, Sippican, and airborne instrumentation carried on-board the NASA DC-8: the NASA/LaRC Laser Atmospheric Sensing Experiment (LASE) DIAL (Differential Absorption Lidar) Lidar system, the LaRC Diode Laser Hygrometer, and the DC-8 cryogenic hygrometer. s used the LASE measurements as the reference. The summary calibration table from a recent analysis of the upper tropospheric calibration these sensor is provided in figure 2, courtesy of Dr. Richard Ferrare of NASA LaRC. The LASE Lidar measurements have been used as the reference in the table.

The table presents the mean upper tropospheric calibration for all sensors involved in the experiment. For this analysis, the upper troposphere was defined as the region from an altitude of 7 km to the tropopause. The conclusion from this analysis is that several instruments agreed within approximately +/-5% of the LASE calibration. Those instruments (in some cases after some iterations in the data analysis as indicated in the table) were the DOE Raman Lidar, the GSFC SRL, the Vaisala RS-80H and the DLH. Both the SnowWhite and the in-situ cryogenic hygrometer on the DC-8 were judged to be significantly dry of LASE and the Sippican significantly wet of LASE. Previous experiments have shown that the Sippican resistive humidity sensor loses the ability to respond to changes in relative humidity (RH) at temperatures below approximately -30C and tends to get "stuck" at too high an RH value. Therefore, the high bias of the Sippican in the final analysis is consistent with earlier studies. While limitations in the cooling capacity of the Peltier cooler and instabilities in the temperature controller have been sited as occasionally limiting SnowWhite measurements [6], other studies have shown good performance of the SnowWhite instrument in the troposphere [7] thererfore no definitive explanation has been given for the mean dry performance of the SnowWhite sensor during AFWEX.

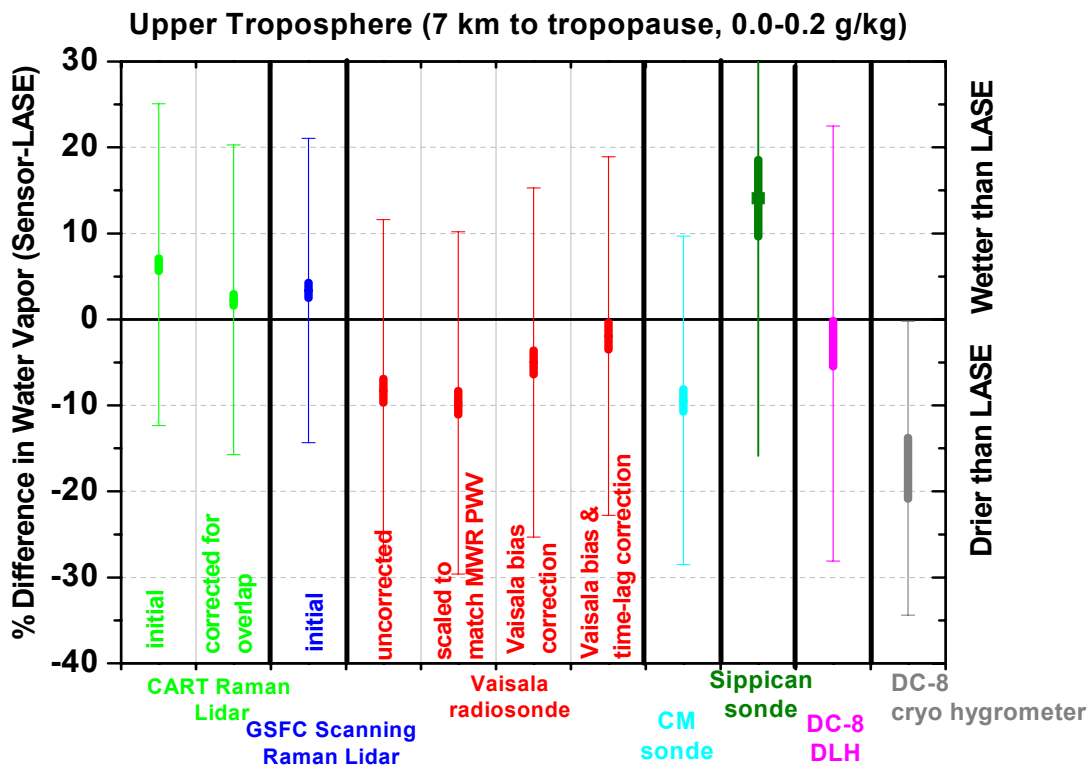


Figure 2: The final upper tropospheric calibration table from the AFWEX field experiment. For this comparison, the LASE airborne DIAL lidar was taken as the reference and the upper troposphere was defined as from 7 km to the tropopause.

4 AIRS Water Vapor Experiment-Ground (AWEX-G)

Therefore, with a history of achieving agreement within ~5% for various upper tropospheric water vapor measurement technologies, the initial proposal for the AWEX-G experiment was to repeat many aspects of AFWEX. The AIRS Water Vapor Experiment-Ground (AWEX-G) was therefore proposed to occur between October 27 - November 16, 2003 with the following goals:

1. Bring a majority of the water vapor measurement technologies in use for AIRS validation together at the ARM SGP site for intercomparison. The period of the experiment would be in the fall when the highest probability of cloud free conditions are found at SGP.
2. Operate these instruments over a three-week period of time in order to characterize the measurement differences of the water vapor technologies and to better understand the existing differences in the AIRS validation measurements.
3. Drawing on ARM experience, determine a standardized radiosonde launch procedure that can be implemented at the AIRS validation sites.
4. Confirm the accuracy of the main ARM SGP water vapor profilers (DOE Raman Lidar and Vaisala RS-90 radiosondes) establishing them as the standards for AIRS validation work. This can be interpreted as bringing the results of the ARM FIRE Water Vapor Experiment (2000) into the AIRS era.

The AWEX-G experiment focused on nighttime radiosonde, Raman lidar, GPS (Global Positioning System) and MWR (Microwave Radiometer) measurements of water vapor. During the experiment 56 balloons carrying 112 radiosonde packages were launched. The radiosonde technologies that were tested were: Vaisala RS80-H, RS90, RS-92, University of Colorado - Cryogenic Frost point Hygrometer (CU-CFH), SnowWhite, Intermet and Sippican. In addition, more than 40 hours of Scanning Raman Lidar measurements of water vapor were acquired in coordination with the radiosonde launches. The DOE CART Raman Lidar (CARL) ran continuously through the experiment as did the CART microwave radiometer and a SuomiNet GPS system that was deployed along with the SRL. Some preliminary results of intercomparison of the AWEX-G instrumentation will be provided here and then a comparison of AIRS fast model calculations with some AWEX-G measurements will be shown. First though is a discussion of the calibration technique that is being used for the water vapor profile data.

4.1 Radiosonde and Lidar calibration with respect to Microwave Radiometer

A standard has developed within the ARM program that the microwave radiometer is used to calibrate the radiosonde and Raman lidar profiles of water vapor by forcing the integrated precipitable water of the profile to match the total column water measured by the radiometer. This is justified based on the work within the ARM effort that has indicated that the MWR is accurate to 3-4% when operating nominally. In AWEX-G, we are attempting to follow this same ARM procedure for profile calibration but at the current time, noise in the radiometers is requiring us to carefully

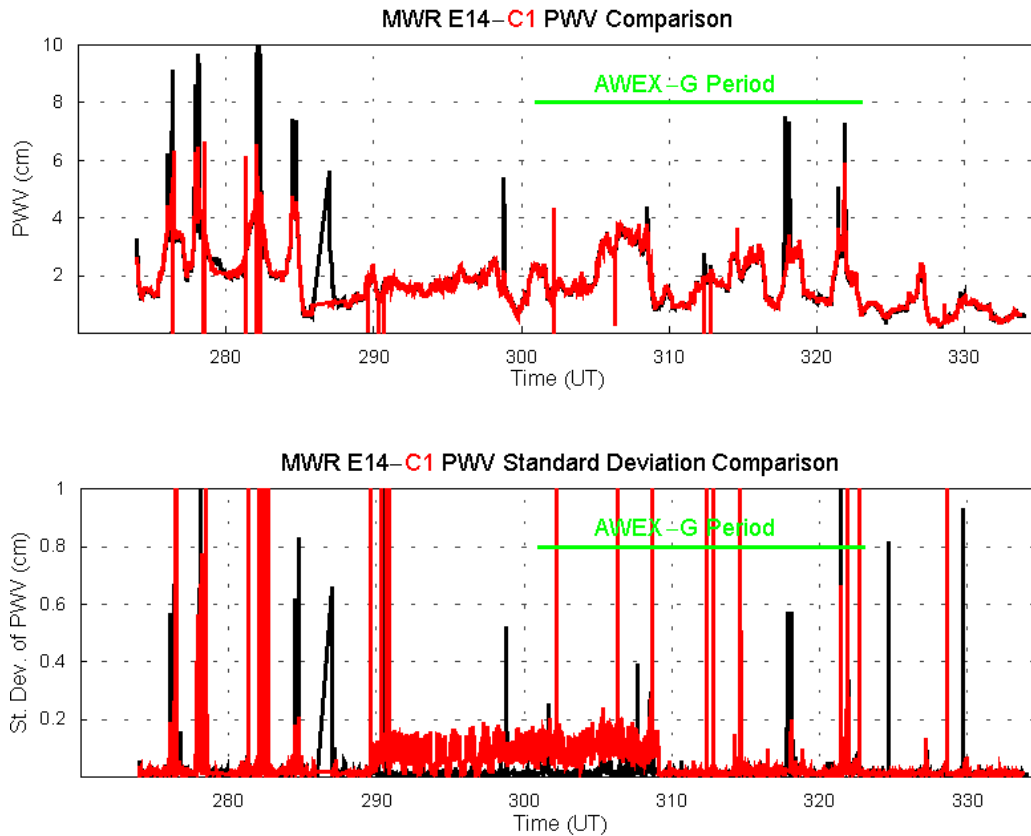


Figure 3: Times series of precipitable water measurements (upper panel) and standard deviation (lower panel) of two MWR instruments at the SGP site during AWEX. Both panels indicate periods of noise and unusually large values of PW that must be culled prior to use for calibration.

study the MWR data themselves. Figure 4 shows a time series of the precipitable water (PW) measurements from the C1 and E14 MWRs that were stationed at the SGP site during AWEX-G.

Several periods of unusually low and high values of PW can be seen in the two-month data record plotted in the top of the figure. In addition, periods of unusually high variance in the data are observed in the lower panel of the figure. These periods are believed to be due primarily to clouds and precipitation. In order to study the MWR data and to determine which radiometer to use as the source of calibration for AWEX-G, different noise filtering schemes are being tested on the data shown in the figure. For example, using a criterion that only values from either C1 or E14 are selected if the values do not differ by more than 25% from each other, figure 4 results.

Although the mean ratio of E14 PW to C1 PW is 1.0, the best fit regression has a slope of 0.975 indicating that the E14 radiometer has 2.5% less sensitivity to changes in PW than the C1 radiome-

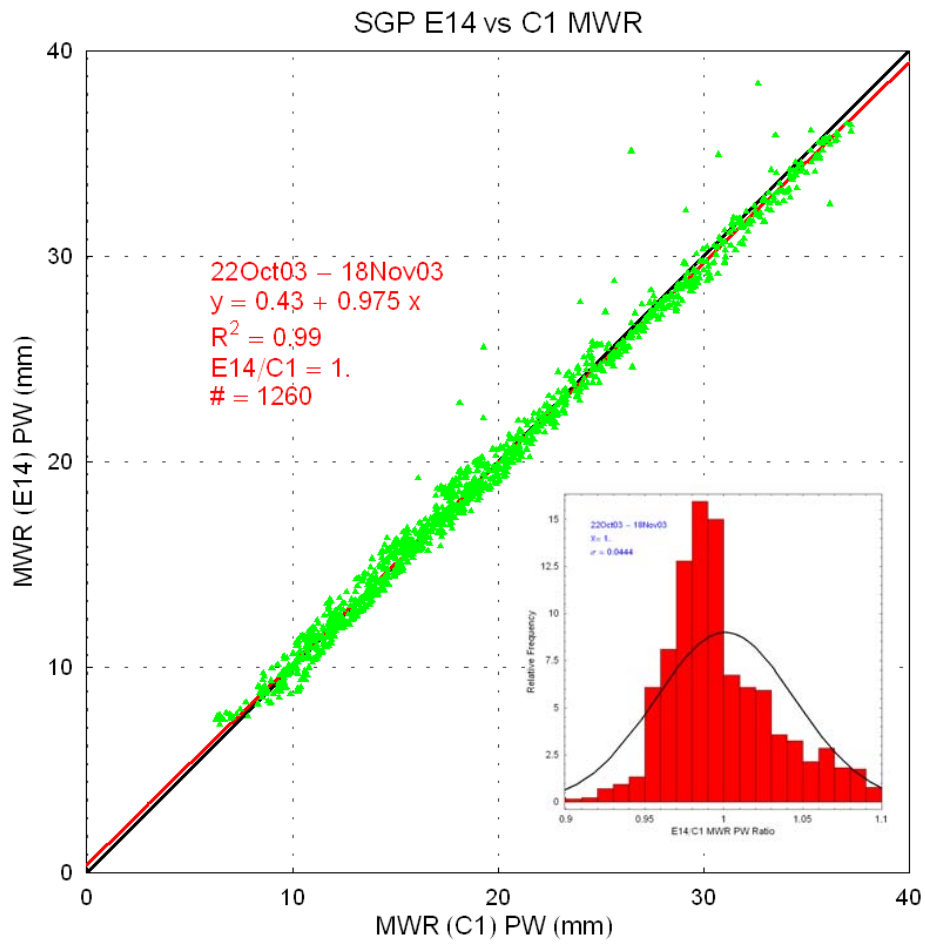


Figure 4: A comparison of PW from C1 and E14 MWR units at the SGP site eliminating points that disagree by more than 25%. Some scatter in the points is still observed with this filtering technique. The histogram exhibits some skewness as well.

ter. There is also a noticeable skewness to the histogram of E14/C1 PW ratios. We will continue to study these radiometer data with the goal of determining an algorithm for data screening that can be used to reject noise spikes even in the absence of other data sources such as second radiometer or a GPS. We would like such an algorithm since part of the AWEX-G activity is to study the use of special radiosonde launches that are being done at the TWP ARM site where only a microwave radiometer is present for PW scaling.

The SuomiNet GPS offers an additional source of precipitable water. The only mobile unit in this international network of GPS systems is deployed in the field with the Scanning Raman Lidar for use in calibration of the lidar. The SuomiNet GPS also was the source of the water vapor calibration for the AIRS comparison measurements shown in figure 1. One of the objectives of AWEX-G was therefore to study the PW values of SuomiNet GPS versus the ARM microwave radiometers. Previous such comparisons have shown a slight dry bias of the GPS with respect to the MWR and have also revealed a diurnal characteristic to the bias. One candidate explanation for the diurnal bias observed in comparisons of GPS and MWR is that the standard GPS processing uses a static atmospheric model for converting the wet delays measured along the line of sight to a satellite to a zenith value. Recently the SuomiNet group at UCAR (University Consortium of Atmospheric Research) has been studying the use of the AVN forecast model in GPS retrievals. Figure 5 shows the comparison of GPS and C1 MWR as a function of time of day using the standard processing software (black) and the updated software using the AVN forecast model (red). The new processing software reduces both the diurnal and overall differences between the GPS and MWR. The GPS PW retrievals using this new processing technique will now be used to help filter out noise in the MWR datasets.

4.1.1 The use of GPS retrievals to filter noise in the MWR data

As an additional source of precipitable water that might be useful in determining which radiometer to use for AWEX-G calibration, figure 6 shows a comparison between the SuomiNet GPS and both the C1 (left) and E14 (right) radiometers. Here again, when the GPS and MWR PW value differed by more than 25% it was not plotted. The mean PW ratios are 0.992 (C1) and 0.994 (E14) and the best fit straight lines have slopes of 0.971 (C1) and 0.995 (E14) revealing essentially the same ~2.5% difference in water vapor sensitivity of the two MWRs shown in figure 4. Both distributions have a reasonably Gaussian appearance. This indicates that the use of the GPS PW retrievals for rejection of MWR noise may be a robust technique for AWEX-G. We will continue to study this as the AWEX-G analysis continues. The analysis that will be presented in the remainder of this report was performed using PW from the C1 radiometer as the calibration source. The analysis will be repeated once an algorithm for selecting which MWR data source is determined.

4.2 Selection of AWEX-G water vapor reference and relationship to AFWEX experiment

The hypothesis that has been taken in the AWEX-G water vapor profile analysis is that the CU-CFH can serve as a stable reference for water vapor with an absolute accuracy of 4-8% throughout its profile. This is based on an analysis performed by Dr. Holger Vömel of the temperature

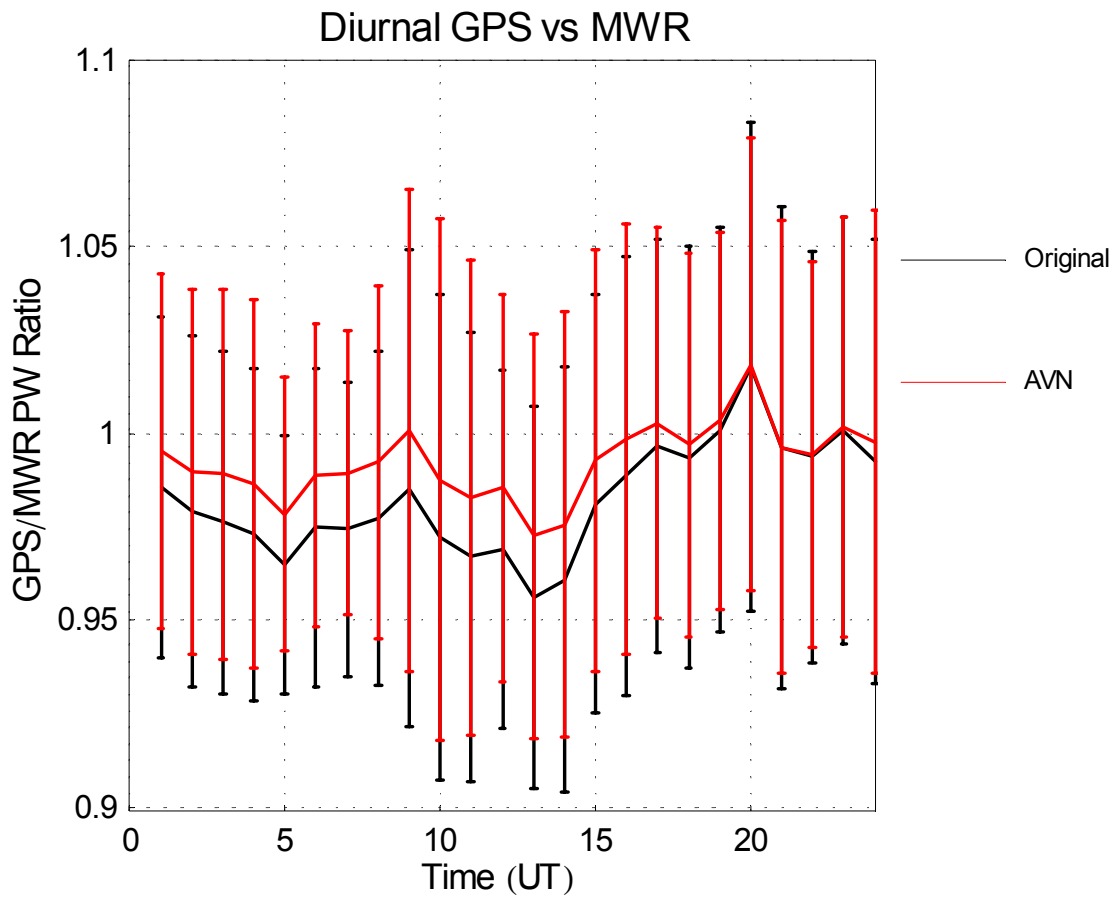


Figure 5: A comparison of GPS and c1 MWR precipitable water measurements where the comparisons have been divided into hourly segments to study diurnal effects. The new processing has reduced the diurnal bias between GPS and MWR.

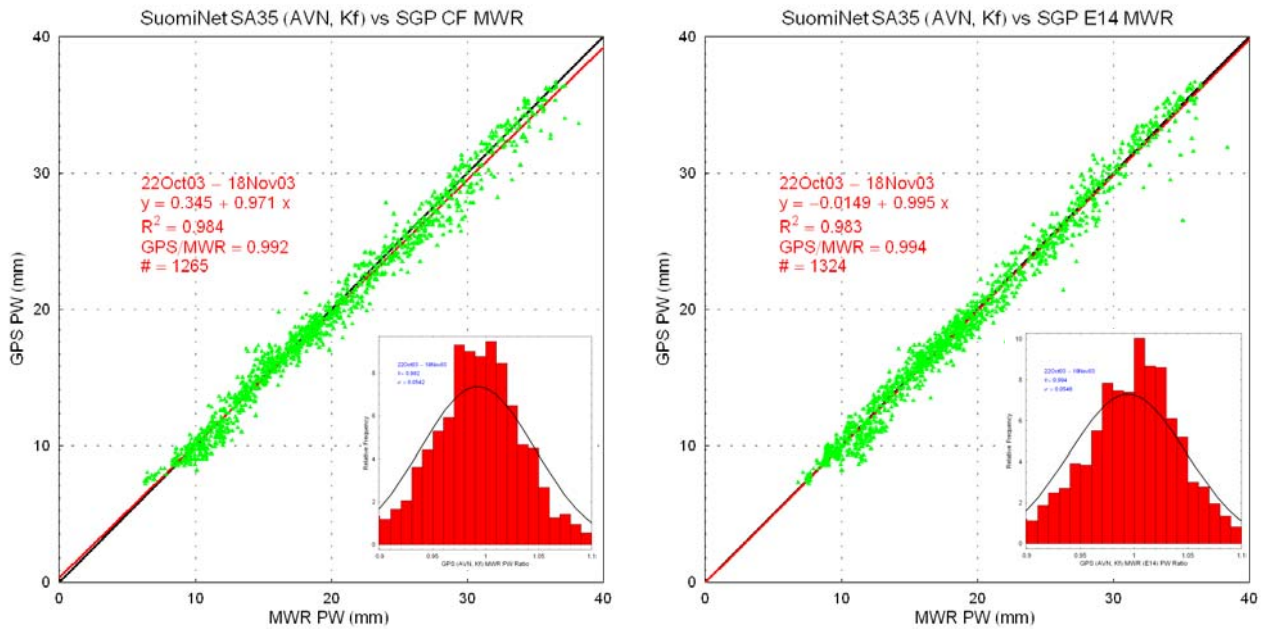


Figure 6: A comparison of the C1 and E14 MWR PW with that derived from SuomiNet GPS using the updated retrieval technique that incorporates the AVN forecast model results in resolving path water vapor measurements to the vertical.

uncertainties of the chilled mirror controller. Thus, on average, the claimed accuracy of CU-CFH the water vapor measurements is approximately the same as that of the Lidar Atmospheric Sensing Experiment (LASE) of LaRC that was used as the reference for the AFWEX upper tropospheric comparisons shown in figure 2. The final analysis of data from AFWEX concluded that the Vaisala RS-80H, CARL lidar, SRL, and the in-situ Diode Laser Hygrometer (DLH) of LaRC were in agreement to within the claimed uncertainties of the LASE instrument ($\pm 6\%$ or 0.01 g/kg of water vapor whichever is larger). We will also compare the final results of AFWEX-G with those of AFWEX by studying the sensors that were involved in both campaigns: the SRL, CARL, Vaisala 80-H and SnowWhite hygrometer. This will permit an indirect study of the hypothesis of the equivalence of CU-CFH and LASE for upper tropospheric water vapor references.

4.3 Characterization of the Vaisala RS-80H and RS-92 with respect to CU-CFH

The initial analysis performed by Dr. Larry Miloshevich on the relative performance of Vaisala RS-80H, RS-92 and CU-CFH is presented in figure 7.

This figure is based on 8 multiple sonde launches involving these three sensors as well as the SnowWhite package. The same data are presented two different ways. The left set of 4 panels presents the analysis in terms of differences in percent RH while the right set of 4 panels is in terms of absolute percentage difference. The RS80-H results are on top and the RS-92 results are on the bottom. It is apparent by visual inspection that the RS-92 measurements were in general much

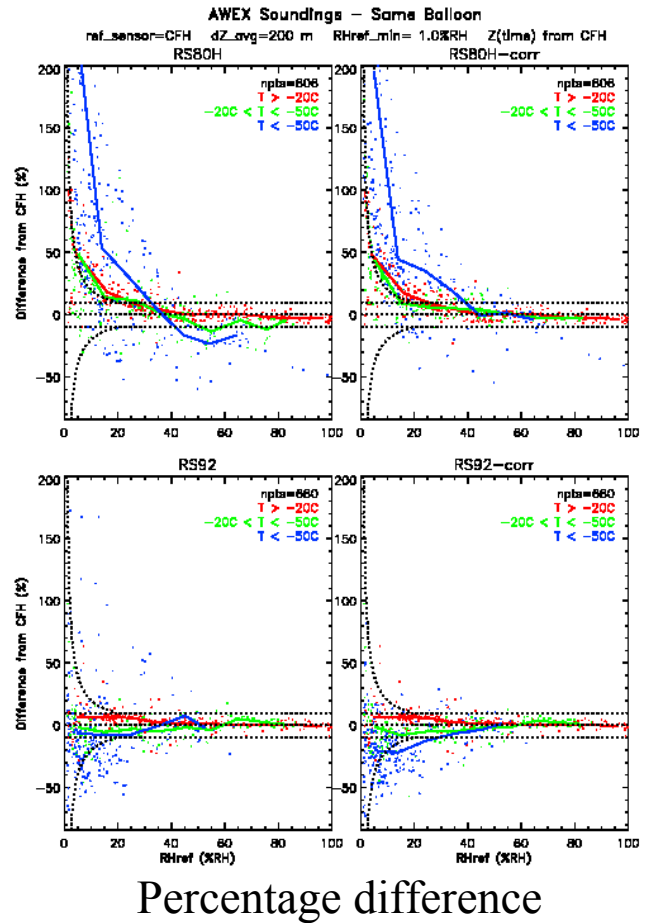
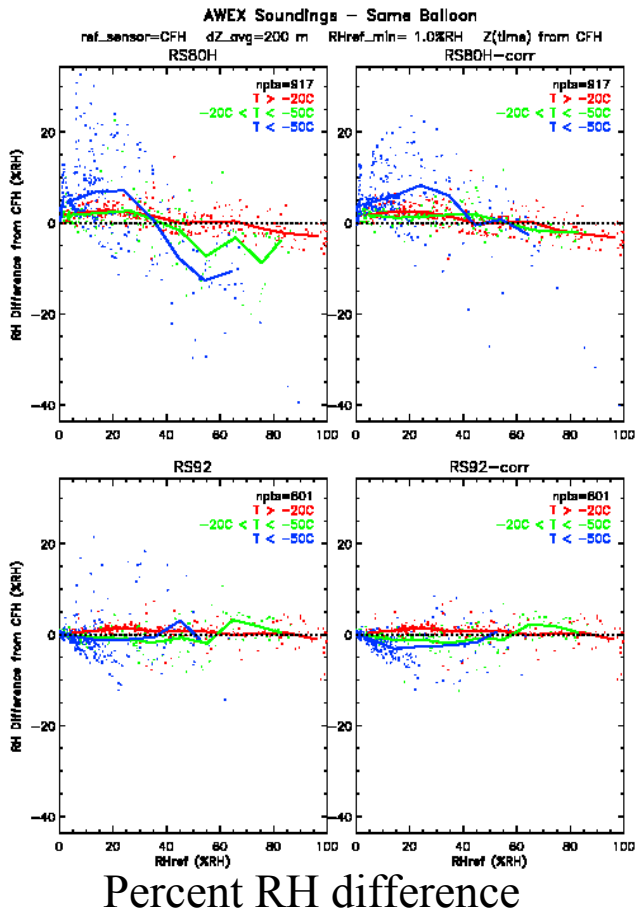


Figure 7: A comparison of Vaisala RS-80H and RS-92 with respect to CU-CFH based on 8 launches on all three packages on the same balloon.

closer to the CU-CFH than the RS-80H. Except at the coldest temperatures (<-50 C) and under conditions of less than 20% RH was the RS-92 in disagreement with the CU-CFH by more than 10%. It should also be mentioned that simultaneous launches of RS-90s and RS-92s performed at AWEX-G indicated that the performance of these two instruments was very similar as expected since they are advertised to share the same humidity sensor. Therefore, we take the comparisons shown in figure 7 for the RS-92 to be representative of the RS-90s as well.

The panel in the upper right of figure 7 shows the RS-80H analysis after time lag correction [3] with differences displayed in terms of percentage difference. This plot indicates errors exceeding 10% for temperatures less than -50 C when the RH was less than $\sim 40\%$. Analysis of the mean UT calibration for the RS-80H during AWEX-G, using a similar approach as used in figure 2 for the AFWEX experiment, indicates a moist bias in the upper troposphere of approximately 20% with respect to CU-CFH. This disagrees with the conclusions drawn from AFWEX for the performance of the RS-80H. In the AFWEX study the mean UT calibration of the RS-80H instrument, after all corrections were applied, was within $\sim 2\%$ of the LASE reference value.

However, a study of the sondes used in AFWEX indicates that the troposphere was considerably drier during AFWEX than during AWEX-G. Most of the AFWEX profiles were characterized by moist layers in the UT that exceeded 40% RH, whereas a large number of the AWEX-G cases had mean UT RH values less than 20%. Referring to the upper right panel in figure 2 shows little bias between CU-CFH for $RH \sim 40\%$ but large wet biases for $T < -50$ C and $RH \sim 20\%$. Given the typically cold temperatures in the upper troposphere, the analysis of figure 2 offers an explanation for an apparent discrepancy between the results of AFWEX and AWEX-G and is an argument in favor of the approximate equivalence of the LASE and CU-CFH as UT references.

4.4 Preliminary Comparison of CART Raman Lidar with sondes

The two permanently stationed water vapor profilers at the DOE ARM SGP site that can potentially provide long term quality data for AIRS comparison are the CART Raman Lidar and the RS-90 radiosonde. One of the explicit goals of AWEX-G was to confirm the utility of these sensors for AIRS validation work. The analysis presented above on the RS-92/90 indicates that the RS-90 data appear to meet this goal. However, unfortunately the preliminary assessment of the CART Raman lidar is that degradations in the performance of this system limit its ability to serve as a useful data source for AIRS. For approximately 18 months prior to AWEX-G, decreases in CARL signal strength have been noted. These have compromised the signal to noise of the instrument. In addition, for reasons that are not known at the current time but will be investigated, a large wet bias has been introduced into the CARL measurements above approximately 6 km. Figure 8 presents comparisons of CARL and two of the radiosondes in use in AWEX-G: the Vaisala RS-90 and CU-CFH. These comparisons both indicate that the CARL lidar goes progressively wet of these two sensors above approximately 6 km.

This same wet bias was observed in the Aerosol IOP held at the SGP site in May, 2003 (Richard Ferrare, verbal communication April, 2004) . The implication is that CARL should probably not be considered as a reliable source of upper tropospheric water vapor data since the launch of AIRS. Considerable effort is currently underway to address the degradations in CARL perfor-

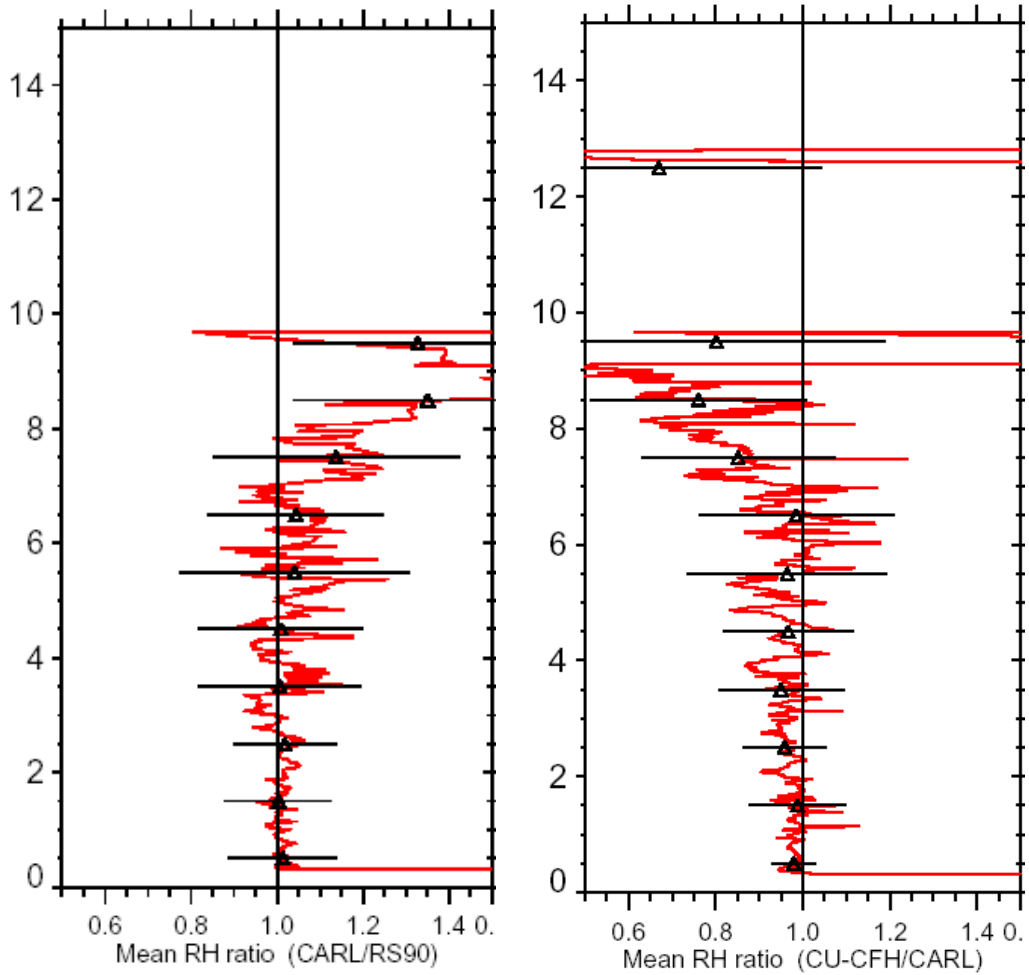


Figure 8: Mean comparison of CARL with RS-90 and CU-CFH radiosondes during AWEX. Note that the CARL data are shown in the numerator on the left and denominator on the right. In both comparisons a significant wet bias is observed in the CARL data above ~6km.

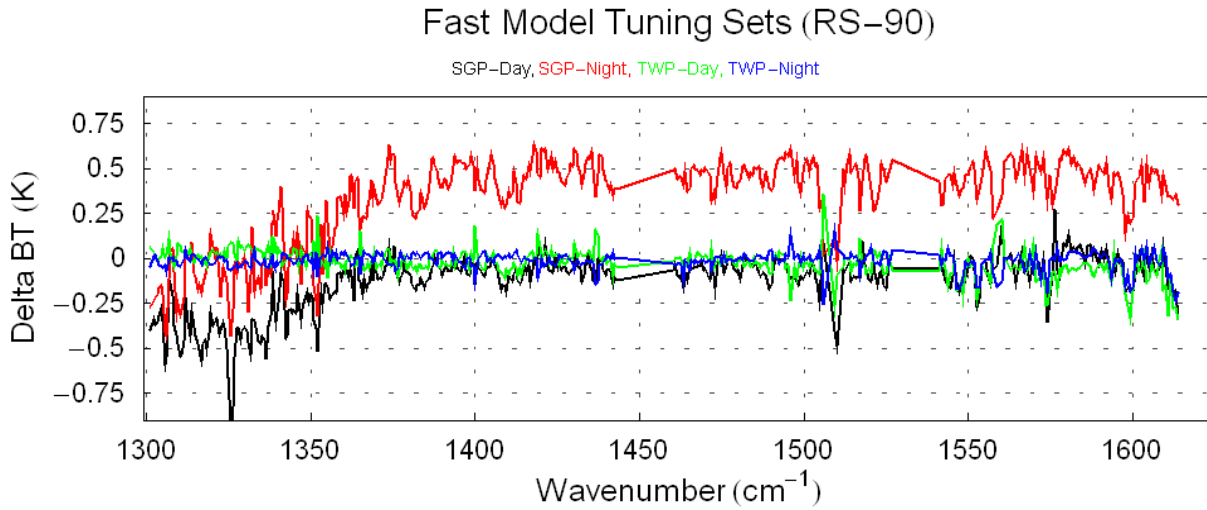


Figure 9: A comparison of AIRS observation and calculations using the AIRS fast model using input data from DOE ARM Tropical Western Pacific and Southern Great Plains sites. The fast model has been tuned to minimize the difference with the TWP data.

mance. There is every expectation that CARL will once again provide quality data of value for AIRS comparisons once it has been refurbished.

4.5 AWEX-G activities relating to AIRS fast model tuning

One of the larger goals of the AWEX-G effort is to work interactively with Larabee Strow's group at UMBC in the validation of the AIRS fast radiative transfer model. At the current time, the fast model channel transmittances have been tuned to minimize the differences between observations and fast model calculations using the best estimate atmospheric product produced by Dr. David Tobin of the University of Wisconsin for RS-90 launches that occurred at the Tropical Western Pacific (TWP) ARM site. Figure 9 presents a comparison of AIRS observations with calculations of the January 2004 version of the AIRS fast model for daytime and nighttime special AIRS RS-90 observations at TWP and SGP.

Individual AIRS channel transmittances have been adjusted in the fast model so as to minimize the differences between the AIRS observations and the calculations of the model using the TWP day and night data sets. It is interesting to note that the calculations based on the nighttime data acquired at SGP also agree very well with the AIRS observations. (The larger differences below 1370 cm^{-1} are thought to be due to contamination of the surface, which is not perfectly characterized in the inputs to the model). The curious outlier is the comparison using the nighttime SGP measurements where a positive offset of $\sim 0.5\text{K}$ exists between observations and calculations. Both AFWEX and AWEX-G were performed at night at SGP so we have a particular motivation to try and resolve the source of this 0.5K difference. There are several items that will be studied to try

and explain this 0.5K difference.

4.5.1 Time lag correction

At the current time, the time lag corrected radiosonde data have not been processed into best estimate products for use in this validation study. We are working on making an assessment of the magnitude of the effect that is created by neglecting this known source of error in the RS-90 data. Work is also in progress to incorporate the time lag correction into future best estimate products from both SGP and TWP.

4.5.2 Cloud clearing

The best estimate profiles have been selected to be as clear as possible based on the AIRS radiances themselves. However, we are involved currently in using both the radiosonde data and cloud mask products created under the ARM program to check for the presence of clouds at the times of the AIRS overpasses. The presence of undetected clouds in an AIRS scene would tend to depress the Obs-Calc result.

4.5.3 ECMWF

The technique that has been used to create the water vapor input to the fast model for the comparisons shown in figure 9 is to use the best estimate product up to 200 mb for water vapor and up to 60 mb for temperature. Above those pressure levels, the ECMWF analysis is used. This is done because of the historically larger uncertainties in radiosonde measurements of, in particular, water vapor at cold temperatures. However, the analysis shown in figure 7 indicate that the RS-90s measurements are within ~10% of CU-CFH for temperatures between -50C and -70C (the lower temperature floor of the AWEX-G dataset) provided that RH is above 20%. The mean tuning sondes profiles are shown in figure 10 indicating that at the TWP the RH on average was above 20% for both daytime and nighttime profiles up to the tropopause.

Considering that temperatures at the tropical tropopause were approximately -80C and that tropopause temperatures at AWEX-G were more typically -70C, and that -70C corresponds to approximately 150mb, we can take the AWEX-G characterization of RS-90 performance to indicate that the RS-90 data are likely useful to higher altitudes in the tropics than is currently being used. Also, the great frequency of supersaturation that exists in the upper troposphere in the tropics must be considered since ECMWF does not permit saturation in its output products. The use of a sub-saturated profile when the atmosphere is actually supersaturated would tend to depress the Obs-Calc result. Therefore, both undetected clouds and also the presence of super saturation conditions that are reported as sub-saturation can depress the Obs-Calc comparison, offering possible explanations for the 0.5K difference observed in figure 9.

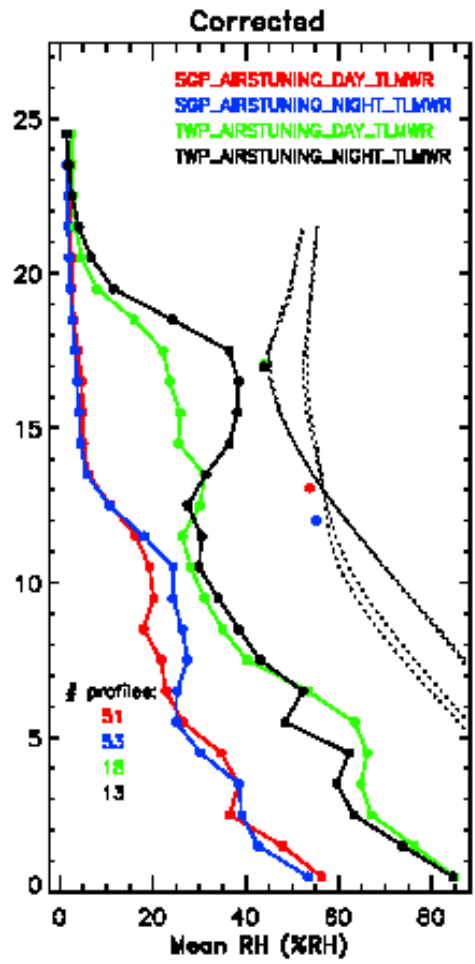


Figure 10: Mean profiles of the radiosonde data used in the comparisons shown in figure 9.

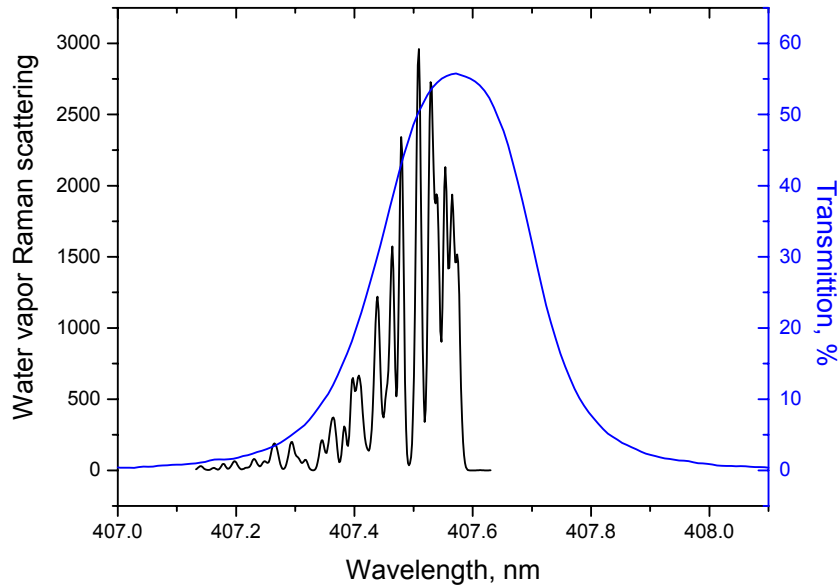


Figure 11: Water vapor filter transmission measurements made at 0.5 cm^{-1} resolution using a Fourier Transform Spectrometer calibrated using a mercury lamp. Also plotted is the Raman water vapor spectrum simulated at 295K.

4.6 Temperature dependence of Raman lidar measurements of water vapor

Raman lidar systems operate by measuring the Raman shifted light scattered from water vapor and nitrogen molecules in the atmosphere. The spectrum of Raman scattering is temperature dependent. Recent work [8] [9] has been done in developing the tools to quantify the influence of this temperature dependence on narrow-band Raman lidar measurements of water vapor such as made by the Scanning Raman Lidar and the CART Raman Lidar. As a part of the AWEX-G effort, these tools have now been used (along with 0.5 cm^{-1} resolution measurements of the water vapor and nitrogen filters used for the SRL measurements during both AFWEX and AWEX-G) to correct the SRL measurements of water vapor mixing ratio. Figure 11 shows the transmission curve of the water vapor filter used in the high SRL channel measured using a Thermo-Electron Nicolet 870 Fourier Transform Spectrometer along with numerical simulations of the water vapor spectrum [1]

The water vapor filter as used in both the AFWEX and AWEX-G field campaigns is not centered on the water vapor feature. Instead figure 11 shows that it is shifted long of the desired spectral location by approximately 0.07 nm. Filter transmission and Raman spectral information are required for both the water vapor filter (shown in figure 11) and the nitrogen filter (not shown) in order to calculate the correction for the influence of atmospheric temperature changes on the water vapor mixing ratio calculation. It must also be true that there are no significant changes in transmission

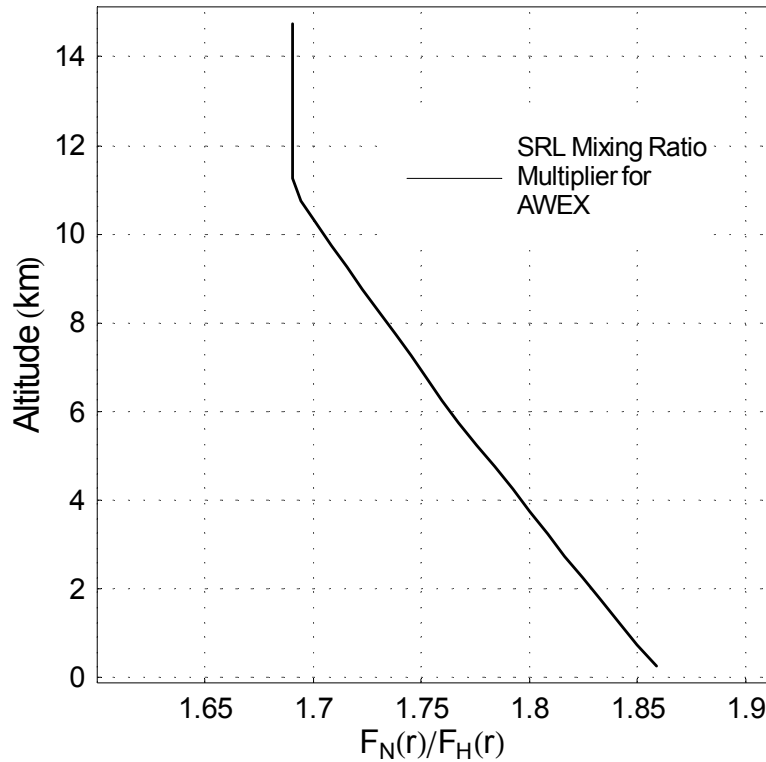


Figure 12: The temperature dependent factor that accounts for the temperature dependence of Raman scattering in the calculation of water vapor mixing ratio is shown for the configuration of the SRL during the AWEX field campaign. The U.S. standard atmosphere has been used for temperature as a function of altitude for this simulation.

across either the water vapor or nitrogen channels introduced by other optics in the lidar system. Assuming the U.S. standard atmosphere, the altitude dependent correction that must be applied to the SRL profile of water vapor mixing ratio is shown in figure 12.

The curve plotted is the ratio of the temperature dependent factors [8] for the measurement of Raman nitrogen ($F_N(r)$) and water vapor ($F_H(r)$). The ratio changes by approximately 10% between the surface and 12 km, a typical upper useful altitude for a 30 minute average of SRL water vapor measurements. This temperature dependence was not accounted for in the analysis presented in figure 1 and is believed to be the explanation for most of the positive bias observed between AIRS observations and fast model calculations shown in that figure.

4.7 The AWEX-G Golden Case - November 19, 2003

AWEX-G was not designed as an activity that would generate a statistically meaningful set of AIRS comparisons. In fact both the weather and an AIRS down period, prompted by a period of

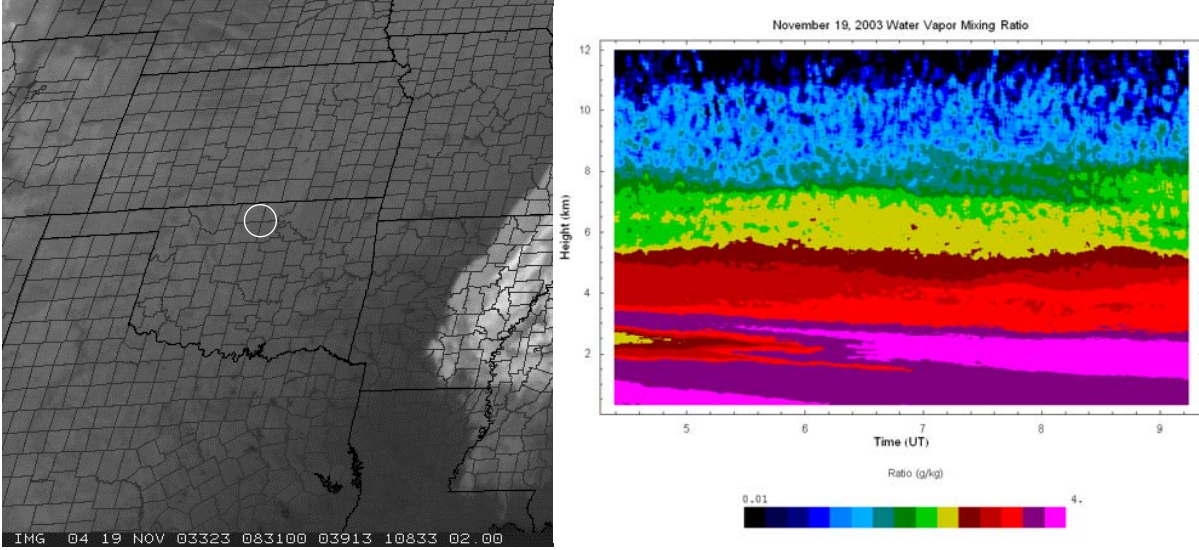


Figure 13: GOES satellite photo at 0831 UT on the night of November 19, 2003 is shown on the left. The location of the SGP site is shown. On the right is the SRL water vapor times series acquired at the SGP site covering the same time period.

solarflare activity, prevented useful AIRS comparisons during much of the experiment. However, as the end of the nominal AWEX-G experiment period approached, it became increasingly apparent that the likelihood of a period of stable and severe clear weather would arrive soon. Because of this forecast, the SRL deployment was extended in order to make measurements during the November 19 AIRS overpass. Figure 13 shows the GOES satellite image at 0831 UT on the left, with the location of the SGP noted, and the SRL water vapor mixing ratio time series on the left. The satellite data, the lidar data and a synoptic analysis indicated that the SGP region was completely clear of clouds. In addition, the SRL time series of water vapor mixing ratio, shown in a log scale to expand the very dry conditions in the upper troposphere, indicates that atmospheric conditions were quite stable during the night. Both of these facts indicate that conditions were optimum for an AIRS comparison. The lack of clouds makes the radiative transfer modeling more straightforward and the relatively stable conditions imply less concern about comparing the measurements from AIRS, where an individual field of view covers 13 km, with either the lidar or the radiosonde that are sampling smaller atmospheric volumes.

4.7.1 Comparison of radiosonde and lidar measurements with AIRS

The comparison of AIRS observations and simulated brightness temperatures using the AIRS fast model using both radiosonde and lidar water vapor data is shown in figure 14. The sae version of the fast model used in the tuning example shown in figure 9 was used here as well. Therefore, this case can be taken as a test of the transmittance tuning derived from comparisons with the TWP validation data.

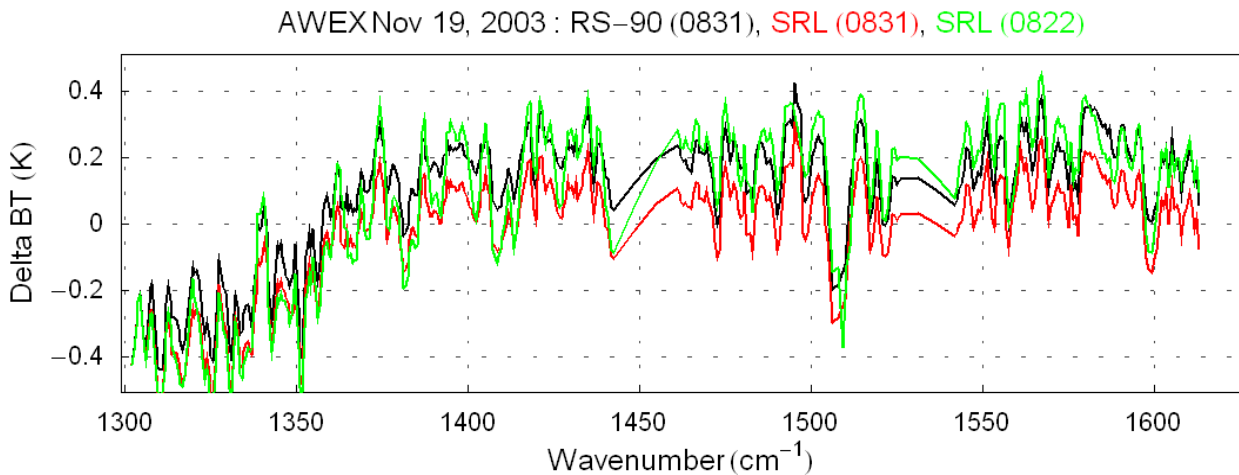


Figure 14: Comparison of AIRS observations at 0822 UT on November 19, 2003 and a radiosonde launched at 0831 and two lidar water vapor profiles: one centered at the AIRS overpass time of 0822 and one centered at the radiosonde launch time of 0831.

The comparison shown in black is that of the AIRS observations at 0822 UT and fast model calculations using the RS-90 radiosonde launched at 0831 UT. There are also two comparisons of AIRS and fast model calculations based on SRL profiles: one centered at the radiosonde launch time of 0831 (red) and the other centered at the AIRS overpass time of 0822 UT (green). Both the radiosonde and lidar data had received only preliminary calibrations at the time of this comparisons, so the results are likely to change slightly in the final analysis, but the agreement in this initial analysis is striking. Above 1370 cm, below which incorrect surface emissivity characterization is believed to be influencing the comparisons, the results agree within $\sim 0.2\text{K}$. Given that the AIRS noise level in the water band has been measured to be about 0.1K , the agreement approaches the noise limit of AIRS. It is just a single comparison between validation data and AIRS, but because of the unusually clear and stable atmospheric conditions and the quality of the calibration source available at the SGP site, the agreement suggests that the recent tuning of the AIRS fast model has greatly reduced the uncertainties demonstrated in figure 1. Preliminary re-analysis of the SRL and sonde data however suggest that the comparisons on the night of November 19 may shift upward closer to the 0.5K bias observed for the SGP nighttime results of the tuning cases shown in figure 9. This emphasizes the need to continue to work toward a resolution of the conspicuous 0.5K difference between day and night SGP datasets studied in the fast model validation activity.

5 Future work

The AWEX-G analysis is not complete. Over the next several months several incomplete research topics will continue to be addressed with a goal of submitting results for publication by the end of 2004. The list of AWEX-G research topics, some of which have not been mentioned previously in this document, that are to be completed in the coming year includes:

- 1) Relate AWEX-G results to those of other experiments such as AFWEX and the three Water Vapor IOPs sponsored by the ARM program
- 2) Draw conclusions about the hypothesis that CU-CFH and LASE are the same UTH standard at the 5% level
- 3) Characterize accuracies of additional sonde packages with respect to CU-CFH using similar analysis as that shown in figure 7. Those sondes include
 - a) SnowWhite
 - b) Internet
 - c) Sippican
- 4) Study the influence of the following factors on the AIRS fast model tuning
 - a) Time lag corrections
 - b) Residual errors in Vaisala calibration functions
 - c) The use of ECMWF as the upward extension of the radiosonde profiles
 - i) Is there a dry bias introduced due to lack of supersaturation in ECMWF?
 - ii) What is the upper useful altitude of the RS-90 data?
- 5) Negotiate with DOE to characterize the CARL lidar channel transmission characteristics so the temperature dependence of the CARL water vapor measurements can be assessed
- 6) Study the influence of different lidar data processing techniques on sonde comparisons
 - a) Straight summation of data using the same temporal window at all altitudes
 - b) Variable temporal summation where the window is expanded as altitude increases
 - c) Shift the data in the upper altitudes according to the ascent rate of the sonde in an attempt to "track" the sonde through the atmosphere
- 7) Study techniques for scaling radiosondes to microwave radiometer
 - a) Should scaling be performed as a multiplier times mixing ratio or as an additive constant in RH space
 - b) Develop noise suppression techniques for processing microwave radiometer data
- 8) Study GPS and MWR PW measurements with the goal of determining a robust algorithm for filtering noisy MWR data
- 9) Perform Mauna Loa Raman Lidar data analysis algorithm comparison

6 Summary

The early AIRS comparison with validation data demonstrated a large uncertainty in the water vapor measurements that were being acquired under this EOS validation activity. This was a

motivator for the AIRS Water Vapor Experiment - Ground (AWEX-G) that took place between October 27 and November, 19, 2003. The main goals of AWEX-G were

1) bring together the main water vapor sensors in use in the AIRS validation activity for inter-comparison and to improve the use of validation data for AIRS purposes

2) re-confirm the utility of the permanently stations water vapor profilers at the SGP, the RS-90 radiosonde and the CART Raman Lidar, as standards for AIRS validation work

Work continues on item 1) above. However a preliminary statement can be made regarding the second and perhaps more important of the two goals listed above. The results presented here indicate that the Vaisala RS-90 can be considered as an accurate source of water vapor data for AIRS comparisons up to the tropopause at SGP and approaching the tropopause at TWP. By contrast, the CART Raman lidar, due to performance degradations that are now being addressed by the ARM program, cannot currently be considered a source of quality water vapor data for AIRS validation. There is every expectation that CARL will again supply quality data of use in AIRS validation once it is refurbished. Numerous other topics are being studied as well with the conclusion of the analysis effort expected by the end of 2004.

7 References

- [1] Avila, G., J. M. Fernandez, B. Mate, G. Tejada, S. Montero, 1999: Ro-vibrational Raman Cross Sections of Water Vapor in the OH Stretching Region, *J. Mol. Spectr.*, **196**, 77-92.
- [2] Ferrare, R. A., E.V. Browell, S. Ismail, S. A. Kooi, L.H. Brasseur, V.G. Brackett, M. B. Clayton, J. D.W. Barrick, G. S. Diskin, J. E.M. Goldsmith, B. M. Lesht, J. R. Podolske, G. W. Sachse, F.J. Schmidlin, D. D. Turner, D. N. Whiteman, D. Tobin, L. M. Miloshevich, H. E. Revercomb, Characterization of upper troposphere water vapor measurements during AFWEX using LASE, submitted to *J. Atmos. Oceanic Tech.*
- [3] Miloshevich, L.M., A. Paukkunen, H. Voemel, and S.J. Oltmans, 2004: Development and validation of a time-lag correction for Vaisala radiosonde humidity measurements. *J. Atmos. Oceanic Technol.* Accepted.
- [4] Revercomb HE, Turner DD, Tobin DC, Knuteson RO, Feltz WF, Barnard J, Bosenberg J, Clough S, Cook D, Ferrare R, Goldsmith J, Gutman S, Halthore R, Lesht B, Liljegren J, Linne H, Michalsky J, Morris V, Porch W, Richardson S, Schmid B, Splitt M, Van Hove T, Westwater E, Whiteman D, The ARM program's water vapor

intensive observation periods - Overview, initial accomplishments, and future challenges, BULLETIN OF THE AMERICAN METEOROLOGICAL SOCIETY 84 (2): 217-236 FEB 2003

- [5] Soden B, Tjemkes S, Schmetz J, Saunders R, Bates J, Ellingson B, Engelen R, Garand L, Jackson D, Jedlovec G, Kleespies T, Randel D, Rayer P, Salathe E, Schwarzkopf D, Scott N, Sohn B, de Souza-Machado S, Strow L, Tobin D, Turner D, van Delst P, Wehr T, An intercomparison of radiation codes for retrieving upper-tropospheric humidity in the 6.3- μ m band: A report from the first GVaP workshop, BULLETIN OF THE AMERICAN METEOROLOGICAL SOCIETY, 81 (4): 797-808 APR 2000

- [6] Vömel H, Fujiwara M, Shiotani M, Hasebe F, Oltmans SJ, Barnes JE, The behavior of the Snow White chilled-mirror hygrometer in extremely dry conditions, JOURNAL OF ATMOSPHERIC AND OCEANIC TECHNOLOGY 20 (11): 1560-1567 NOV 2003

- [7] Wang JH, Carlson DJ, Parsons DB, Hock TF, Lauritsen D, Cole HL, Beierle K, Chamberlain E Performance of operational radiosonde humidity sensors in direct comparison with a chilled mirror dew-point hygrometer and its climate implication, GEOPHYSICAL RESEARCH LETTERS 30 (16): Art. No. 1860 AUG 27 2003

- [8] Whiteman, David N., 2003: Examination of the traditional Raman lidar technique. I. Evaluating the temperature-dependent lidar equations, Applied Optics, 42, No. 15, 2571-2592.

- [9] Whiteman, David N., 2003: Examination of the traditional Raman lidar technique. II. Evaluating the ratios for water vapor and aerosols, Applied Optics, 42, No. 15, 2593-2608